Nuclear structure and decay modes of Ra isotopes within an axially deformed relativistic mean field model*

Rashmirekha Swain[1;1)] S. K. Patra[2] B. B. Sahu[1;2)]

[1] School of Applied Sciences, KIIT Deemed to be University, Bhubaneswar-751024, Odisha, India
[2] Institute of Physics, Bhubaneswar- 751005, India

Abstract: We examine the structural properties and half-life decay of Ra isotopes within the axially deformed Relativistic Mean-Field (RMF) theory with NL3 force parameters. We work out the binding energy (BE), RMS radii, two-neutron separation energies (S_{2n}), and some other observables. The results are in good agreement with the finite-range droplet model (FRDM) and experimental results. Considering the possibility of neutron magic number, the α-decay and cluster decay half-lives of Ra isotopes are calculated systematically using the Q-values obtained from the RMF formalism. These decay half-life calculations are carried out by taking three different empirical formulae. The calculated decay half-lives are found to be highly sensitive to the choice of Q-values. Possible shell or sub-shell closures are found at daughter nuclei with $N = 128$ and $N = 126$ when alpha and ^{8}Be, ^{12}C, ^{18}O respectively are emitted from Ra isotopes. Though the cluster radioactivity is affected by the shell closure of parent and daughter, a long half-life indicates the stability of the parent, and a small parent half-life indicates that the shell stability of the daughter against decay.

Keywords: relativistic mean field, nuclear bulk properties, alpha and cluster decay half-life

PACS: 21.10.Dr, 21.10.Ft, 21.10.Gv **DOI:** 10.1088/1674-1137/42/8/084102

1 Introduction

Heavy and super-heavy nuclei are in general dynamically unstable. Energy is gained by breaking the nucleus into two component parts. However, some heavy nuclei decay by quantum-mechanical leakage through the potential barrier. A number of theoretical and experimental studies have been carried out on the decay modes of heavy and super-heavy nuclei, like alpha decay, beta decay and gamma decay preceded by the synthesis of heavy and super-heavy nuclei far away from the stability line [1–11]. The discovery of new exotic decay modes of nuclei, starting from double beta decay, proton decay, and cluster radioactivity to beta delayed particle emission, like the isotopes of C and O, leads to possible shell or sub-shell closures at parent or daughter nuclei as the outcomes of these studies [12–22]. Since the main decay modes of heavy and super-heavy nuclei are alpha decay and spontaneous fission, one should have a thorough understanding of the dominant decay mode of heavy and super-heavy nuclei in order to produce artificial super-heavy nuclei. The investigation of alpha decay has become a very interesting research topic in recent years, as it provides useful content about the shell and sub-shell structure of the parent nuclei. Moreover, alpha decay half-lives are used to search for new super-heavy elements synthesized at labs such as Berkeley, GSI, and Dubna [23, 24]. The alpha decay mechanism [25, 26] has been explained theoretically by the quantum mechanical tunneling process. Gamow established a logical relationship between half-lives and decay energies, which was found empirically by Geiger and Nuttall [27]. Features of alpha decay are: (i) its properties (together with γ-spectroscopy) are a probe to establish nuclear levels (excitation energies, spin and parity assignments); (ii) it is a probe for (long lived) isomeric states; (iii) $\alpha-$decay energies are a measure for mass excesses; (iv) it is an (indirect) measure for stability against SF; (v) $\alpha-$decay energies are a sensitive probe to detect nuclear shells; (vi) it is easy to detect with high efficiency; and (vii) it is one boundary for the stability and thus the existence of super-heavy nuclei. Compared to alpha decay, the situation in spontaneous fission is very analyzable. In addition to the release of energy, there are large number of foregone conclusions in the fission process, such as mass, the number of emitted neutrons, charge number of the two fragments etc, predicted first in 1980 by Sandulescu et al. [1], with alpha decay theory extending to

Received 22 April 2018, Published online 9 July 2018
* Supported by Project No. SR/FTP/PS-106/2013, SERB, DST, Govt. of India
1) E-mail: rashmirekhaswain16@gmail.com
2) E-mail: bbsahufpy@kiit.ac.in

heavier fragments [28] in 1985. Another possible decay is beta decay. Compared to alpha decay and spontaneous fission, the slow and little favoured beta decay process takes place via the weak interaction. Nuclei with comparatively longer half-life for spontaneous fission against beta decay might decay via alpha emission. So heavy or super-heavy nuclei which have a short alpha decay half-life compared to spontaneous fission half-life will undergo fission and can be detected in the laboratory through alpha decay. After the discovery of cluster radioactivity of Ra isotopes by Rose and Jones [29], a brand-new field of research was opened in nuclear physics. This experimental result was conformed by Gales [30] and Price et al. [31]. These exotic decay processes have motivated us to focus on their structures and the decay modes of Ra isotopes in the theoretical account of the RMF model, since the time when the structure of octupole deformed isotopes been determined [32].

The major purpose of the present study is to examine the α and cluster decay processes in the region of $A{\sim}220$ to predict the existence of spherical shell/sub-shell closures in the daughter lead region within an axially deformed relativistic mean field (RMF) theory. Especially, in the field of exotic cluster decays, the study of radium isotopes is essential because of their location in the nuclear chart, which lead to the formation of stable lead isotopes.

It is clear that cluster radioactivity is related to shell/sub-shell closure, so it is very important to evaluate how much the shell effects impart to the half-life for α and cluster radioactivity. This is the primary motivation for this work. Again, the mass region of $A{\sim}220$ is crucial because there is strong specific evidence that in certain heavy and/or super-heavy regions, octupole-deformed atomic nuclei are distorted into a pear shape [32]. Strong octupole configurations with opposite parity lead to pear shapes when the nucleons of rotational states near the Fermi surface populate E1 and electric-octupole (E3) transition moments. A detailed understanding of the structures of these nuclei is essential to get direct content on octupole correlations with these nuclei [32]. So, to provide a little information in this regard, we study the half-life of these nuclei. Along with this we have examined the bulk properties of the isotopes of Ra using RMF theory. Although in this mass region, detailed spectroscopic study of these nuclei is also needed, we have confined ourselves only to the study of the bulk properties of Ra isotopes, though some of our collaborators have studied the spectroscopic properties earlier in Refs. [33, 34] for Sm and Er isotopes. Here we focus on the study of bulk properties of the nuclei in the mass region of $A{\sim}200-230$ using RMF theory. The RMF model is very useful not only to explore the ground state properties of nuclei [35, 36] in the line of stability, but can also be extended to drip line nuclei. The results of this model, such as the knowledge of rms radii of neutron-rich nuclei and hence the neutron halos, remain a current theoretical and experimental research topic. Toki et al. [37] have studied the neutron and proton radii of nuclei up to the drip line without changing other gross properties which are insusceptible to the ρ-meson coupling strength. Their results show some sensitivity to the ρ-meson coupling, which is intrinsically incorporated in our RMF model used here.

Rose and Jones first discovered the radioactive decay of ^{14}C experimentally from ^{223}Ra [29]. Soon after that, many cluster radioactivity decays from heavy nuclei were observed and studied [19, 38–47]. Santhosh et al analysed the exotic decay and the fine structure of Ra isotopes using a fission-like model, considering the interacting potential as the sum of proximity and Coulomb potentials, and got some important results [48, 49]. The Super-Asymmetric Fission Model (SAFM) [50], Preformed Cluster Model [51] and many other models have been utilised to study the several ascertained exotic cluster radioactivity decays [52–55]. Recently, however, the role of deformations and orientations of nuclei has been studied in cluster decays of different radioactive nuclei decaying to a doubly closed spherical shell [56]. The effect of impairment on half-lives of exotic cluster decays was studied in Refs. [57–60]. The taxonomic cluster radioactivity study of $^{210-226}$Ra nuclei has also been examined within an axially deformed RMF theory and $^{210-226}$Ra found to be alpha unstable (and therefore possess α radioactivity) [55, 61, 62].

In our present study, using the RMF model we study the bulk properties of Ra isotopes with a NL3 force parameter set [63]. This has been used successfully to describe the ground state properties of nuclei in the line of stability, distorted and exotic nuclei [63, 64]. The Q-value is obtained from the binding energies of the nuclei. With this Q-value we examine the α-decay as well as cluster decay half-life of Ra isotopes using the Viola-Seaborg [65], Royer [66, 67], universal decay law [68, 69], and the universal formula (Univ) of Poenaru et al. [50]. Along with the structural study of Ra isotopes, we also show how the half-lives are sensitive to the shell closures of parent and daughter nuclei.

The rest of this paper is structured as follows. In Section 2 we give a concise description of the RMF formalism. The results obtained are presented in Section 3, and a summary of the results with concluding remarks is given in Section 4.

2 Theoretical framework

2.1 Relativistic Mean Field (RMF) formalism

The concept of a relativistic description of nuclear systems was raised in the 1950s, by Schiff [70], Teller and Durr [71, 72]. The idea further developed when Miller and Green, and then Walecka [73], pointed out the simple form of the interaction of nucleons through mesons with few degrees of freedom [35]. This model is developed within the framework of quantum hydrodynamics (QHD). There are four basic assumptions behind this theory: (i) the nucleons are considered as point particles; (ii) nucleons are the effective degrees of freedom at low energy and they are included as Dirac spinor ψ_i; (iii) these particles conform stringently to the rules of relativity and causality; and (iv) the theory is minimally Lorentz invariant. The other degrees of freedom are non-Goldstone bosons or mesons such as σ, ω, ρ and δ. One of the main interesting attributes of this model is that the inclusion of spin-orbit strength subordinated nuclear shell structure mechanically develops from the nucleon-nucleon interaction [35, 74]. The basic ingredient for a nucleon-meson many-body system is the relativistic Lagrangian density [35, 75–80]:

$$\begin{aligned} L = & \bar{\psi}_i(i\gamma^\mu\partial_\mu - M)\psi_i + \frac{1}{2}\partial^\mu\sigma\partial_\mu\sigma - \frac{1}{2}m_\sigma^2\sigma^2 \\ & -\frac{1}{3}g_2\sigma^3 - \frac{1}{4}g_3\sigma^4 - g_s\bar{\psi}_i\psi_i\sigma - \frac{1}{4}\Omega^{\mu\nu}\Omega_{\mu\nu} \\ & +\frac{1}{2}m_\omega^2 V^\mu V_\mu + \frac{1}{4}c_3(V_\mu V^\mu)^2 - g_\omega\bar{\psi}_i\gamma^\mu\psi_i V_\mu \\ & -\frac{1}{4}\overrightarrow{B}^{\mu\nu}.\overrightarrow{B}_{\mu\nu} + \frac{1}{2}m_\rho^2\overrightarrow{R}^\mu.\overrightarrow{R_\mu} \\ & -g_\rho\bar{\psi}_i\gamma^\mu\overrightarrow{\tau}\psi_i.\overrightarrow{R^\mu} \\ & -\frac{1}{4}F^{\mu\nu}F_{\mu\nu} - e\bar{\psi}_i\gamma^\mu\frac{(1-\tau_{3i})}{2}\psi_i A_\mu, \end{aligned} \tag{1}$$

where all the symbols have their usual meaning. We derive the field equations from the above Lagrangian for the nucleons and mesons. With the expansion of Dirac spinors and the boson fields in an axially deformed harmonic oscillator basis, a set of coupled equations is solved numerically by a self-consistent iteration method with an initial deformation value β_0 [36]. The customary harmonic oscillator formula for the center-of-mass energy correction is given by $E_{\text{c.m.}} = \frac{3}{4}(41A^{-1/3})$. The quadrupole deformation parameter β_2 is evaluated from the proton and neutron quadrupole moments, as $Q = Q_\text{n} + Q_\text{p} = \sqrt{\frac{16\pi}{5}}(\frac{3}{4\pi}AR^2\beta_2)$. The rms matter radius is obtained as $<r_\text{m}^2> = \frac{1}{A}\int\rho(r_\perp,z)r^2\text{d}\tau$, where $\rho(r_\perp,z)$ is the deformed density and A is the mass number.

Since the RMF automatically considers the spin orbit interaction, it receives much attention due to its spectacular achievements in describing the structure of stable nuclei [81], proton-rich nuclei [82], neutron-rich nuclei [83], superdeformed nuclei [84], and superheavy nuclei [84–88]. In addition to this, RMF theory has developed in many directions in recent years [89–91]. In the low energy regime it is now a standard tool to study the nuclear structure.

The pairing phenomenon is a very important quantity for determining the nuclear properties in open shell nuclei. The pairing correlations are taken care of by the Bardeen-Cooper-Schrieffer (BCS) method. We use a constant gap for the proton and neutron in order to deal with the pairing effects, as given in Refs. [92, 93]: $\Delta_\text{p} = RB_s\text{e}^{sI-tI^2}/Z^{1/3}$ and $\Delta_\text{n} = RB_s\text{e}^{-sI-tI^2}/A^{1/3}$ with R=5.72, s=0.118, t=8.12, B_s=1 and $I=(N–Z)/(N+Z)$. This type of pairing effect has already been used the other authors [80, 94] and reported in Ref. [80, 94]. The obtained results for binding energies are identical with those of the relativistic Hartree-Bogoliubov formulations. The total binding energy (BE) and other observables are obtained by using the standard relations, as given in Ref. [76, 77].

2.2 Viola-Seaborg calculation

The semi-empirical Viola-Seaborg relation, with the constants ascertained by Sobiczewski et al. [95], is written as,

$$\log_{10} T_{1/2} = (aZ+b)Q^{-1/2} + cZ + d + h_{\log}. \tag{2}$$

Here Z is the atomic number of the parent nucleus and the Q-value is in MeV. The parameters a, b, c, and d are constants with a = 1.66175, b = −8.5166, c = −0.20228, and d = −33.9069. The quantity $h_{\log}$ represents the deterrent which is associated with the odd-odd proton and neutron numbers, given by the Viola-Seaborg formula. Here we have taken the hindrance factor as:

$h_{\log}$=0, for Z, N even,

$h_{\log}$=0.772, for Z=odd, N=even,

$h_{\log}$=1.066, for Z=even, N=odd,

$h_{\log}$=1.114, for Z, N odd.

2.3 Universal decay law (UDL)

Thomas developed the decay width expression of cluster radioactivity by evaluating the residues of the corresponding S matrix in the theoretical account of the R-matrix [96, 97]. The decay half-life can be written in the form

$$\log_{10} T_{1/2} = aZ_eZ_d\sqrt{\frac{A}{Q_e}} + b\sqrt{AZ_eZ_d(A_d^{1/3}+A_e^{1/3})} + c, \tag{3}$$

$$\log_{10} T_{1/2} = a\chi' + b\rho' + c. \tag{4}$$

This formulation links up the monopole radioactive decay half-life with the Q-values of out-flowing particles as well as the charges and masses of the nuclei involved in the decay. Here the cluster Q-value is $Q_e = \mu\nu^2/2$ and

the standard value of $R=R_0(A_d^{1/3}+A_e^{1/3})$ with $R_0\sim1.2$ fm [98, 99].
The factors χ' and ρ' are defined as,

$$\chi'=\frac{\hbar}{e^2\sqrt{2m}}\chi=Z_eZ_d\sqrt{\frac{A}{Q_e}},$$

$$\rho'=\frac{\hbar}{\sqrt{2mR_0e^2}}(\rho\chi)^{1/2}=\sqrt{AZ_eZ_d(A_d^{1/3}+A_e^{1/3}},$$

where $A=A_dA_e/(A_d+A_e)=\mu/m$ and m is the nucleon mass.The constants $a=0.3671$, $b=-0.3296$ and $c{=}-26.2681$ are the co-efficient set.

2.4 Royer analytical formulae

Analytical formulae for the decay half-lives of alpha radioactivity were derived by G. Royer. A simple analytical logarithmic half-life formula for the heavy elements is obtained with a rms deviation of 0.42 [100] and used here:

$$\log_{10}[T_{1/2}(s)]=-26.06-1.114A^{1/6}\sqrt{Z}+\frac{1.5837Z}{\sqrt{Q_\alpha}}, \quad (5)$$

where A is the mass number and Z is the charge number of the parent nucleus. Q_α represents the energy released during the reaction. The constants a, b and c for different configurations of Z and N are shown in Table 1.

Table 1. Constants used in the Royer formula.

Z	N	a	b	c
even	even	-25.31	-1.1629	1.5864
even	odd	-26.65	-1.0859	1.5848
odd	even	-25.68	-1.1423	1.5920
odd	odd	-29.48	-1.1130	1.6971

2.5 Universal curve (Univ) formula

The cluster decay half-life calculations are also done using the universal formula (Univ) of Poenaru et al. [50], given as:

$$\log_{10}\ T_{1/2}(s)=-\log_{10}\ P-\log_{10}\ S+[\log_{10}(\ln2)-\log_{10}\ \nu]. \quad (6)$$

Here ν is a constant frequency and S is the preformation probability of the cluster, which depends upon the mass number of the emitted cluster. The decimal logarithm of the preformation factor is given by,

$$\log_{10}\ S=-0.598(A_e-1). \quad (7)$$

The additive constant for an even-even nucleus is written as

$$C_{ee}=[-\log_{10}\ \nu+\log_{10}(\ln2)]=-22.16917. \quad (8)$$

Here the Q-value is calulated analytically.

$$-\log_{10}P\ =\ 0.22873(\mu_AZ_dZ_eR_b)^{1/2} \times[\arccos(\sqrt{r}-\sqrt{r(1-r)})], \quad (9)$$

where μ is the reduced mass, $r=R_t/R_b$, $R_t=1.2249(A_d^{1/3}+A_e^{1/3})$, $R_b{=}1.43998\ Z_d\ Z_e/Q$.

3 Results and discussion

Here, the numerical computations have been carried out using the maximum oscillator shell $N_{\rm F}=N_{\rm B}=16$ for fermions and bosons. To solve this standard RMF Lagrangian there exist a number of force parameter sets. In this work, we have used the NL3 parameter set [63], which has previously been successfully used in various mass regions [35, 36]. The measurement/study of the mass of atomic nuclei is fundamental both in the mean nuclear field and nucleon- nucleon correlations and the study of other bulk properties highly pertinent for understanding various attributes of the nuclear structures.

Binding energy (BE) is one of the fundamental observables used to determine the stability of a nucleus. In this regard we have calculated the BE per particle (BE/A) for $^{210-226}$Ra using RMF with the NL3 force parameters. The obtained outcomes are compared with finite-range droplet model (FRDM) and experimental results [101, 102] wherever available, as shown in Fig. 1. From the figure we observe that BE/A shows the usual behaviour with the increase of mass number and reaches a reproductive structure value at $N\sim126$ $(A=214, Z=88)$, then decreases gradually towards the higher mass region. This means that ^{214}Ra is the most stable element from the binding energy viewpoint. Similar results are also obtained from the FRDM and the National Nuclear Data Center (NNDC).

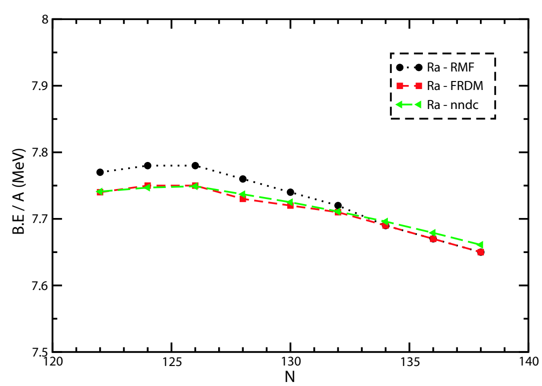

Fig. 1. (color online) The binding energy per particle (BE/A) calculated from RMF(NL3) (circles) are compared with FRDM [101] (squares) and experimental (LHT) [102] values for Ra isotopes.

Here we study the alpha decay and cluster decay half-lives of Ra isotopes $(Z=88)$ by using the RMF formalism with different formulae such as Viola-Seaborg semi-empirical (VSS) model, Royer's analytical formulae, the universal decay law (UDL), and the universal formula

(Univ) of Poenaru et al. We also compare the obtained alpha and cluster decay half-lives with the experimental value wherever available, and with the results from other models found in the literature [47].

The root mean square (rms) radius for neutrons (r_n), for protons (r_p), and the total or matter radius (r_m) are obtained in the RMF model by using the NL3 force parameter set, with the results shown in Fig. 2. The neutron radius (r_n) increases with the increase of neutron number when the proton number is constant ($Z=88$). Similar things happens for the matter radius. This change is significant and involves as a necessary consequence the existence of more neutrons near the surface, satisfying the work done by Iversen et. al [103] that r_n - r_p = 0.03(3) fm. The excess neutrons are accessible in the surface of heavy nuclei [104]. The difference is incurred because of the elastic scattering of these valence neutrons. Again, the optical model analysis of elastic scattering is purely a surface phenomena [105], hence the difference. The modification of proton rms radii is more gradual than that of the neutron and matter rms radii. From Fig. 2, the root mean square values gradually increase until $A=270$ ($N=182$). A jump is found at $A=229$ ($N=141$), which may be due to the scattering of low-lying resonances of small angular momentum with the Cooper pairs of the continuum and/or the recently studied odd-even effect of the density-dependent pairing force which vanishes around N $\sim$ 2Z [106]. There is no data or any other calculations for comparison.

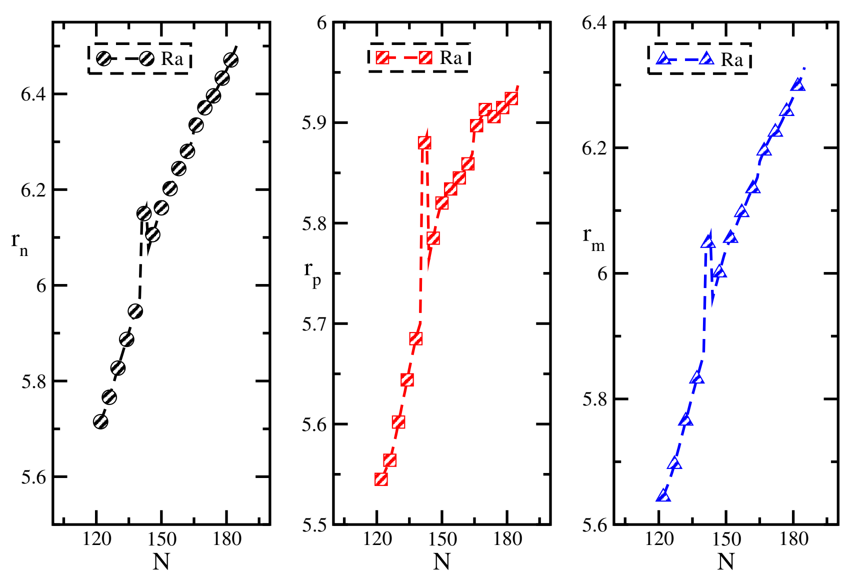

Fig. 2. (color online) The rms radii of neutron (r_n), proton (r_p) and matter (r_m) distributions for $^{210-270}$Ra isotopes using relativistic mean field formalism RMF(NL3).

Within a rich collective phenomenology, the two-neutron separation energies are obtained from the calculated binding energies of Ra isotopes. These are related to structural phenomena like shell and sub-shell closures. In order to make our study more realistic, S_{2n} has been examined and shown in Fig. 3, and the differential variation of S_{2n} in Fig. 4. S_{2n} can be written as,

$$S_{2n}(N,Z)=BE(N,Z)-BE(N-2,Z). \qquad (10)$$

The differential variation of S_{2n} with respect to the parent neutron number i.e. $dS_{2n}(Z,N)$, can be written as,

$$dS_{2n}(Z,N)=\frac{S_{2n}(Z,N+2)-S_{2n}(Z,N)}{2}, \qquad (11)$$

$dS_{2n}(Z,N)$, shown in Fig. 4, is a very important factor to find the rate of change of separation energy in an isotopic chain with respect to the parent neutron number. Here we calculate $dS_{2n}(Z,N)$ and compare our results with FRDM and experimental results [101, 102]. We notice a major shell closure at $N=128$. In addition to this, dS_{2n} clearly shows non-linear behavior at $N=132/134/136$. It conveys a possible phase/shape transition [107] and its dependence on proton number is reflected in the behaviour of S_{2n}. The two neutron separation energies and their evolution with neutron number are a very good beginning point for investigating various nuclear structure models.

It is found from Table 2 that the half-life is small for the parent nucleus ^{218}Ra as per the VSS, Royer and UDL formalism with Q-value of 9.038 MeV. Hence the possible shell is stabilized at the daughter nucleus ^{214}Rn when an α particle is emitted from the ^{218}Ra nucleus. However, the experimental half-lives show the shell stabilization at the ^{212}Rn daughter nucleus. On the other hand we found a remarkably larger half-life with the VSS, Royer and UDL formalism in the case of ^{212}Ra, clearly showing the shell stabilization. From Table 3 it is observed that when ^{8}Be is emitted from Ra isotopes, the half-life is small for the ^{218}Ra nucleus compared to other isotopes for both the calculated and experimental Q-values, given in the fourth and sixth column respectively using the same UDL formalism, which may indicate possible shell and/or sub-shell closure at ^{210}Po. Again, larger half-life is shown at ^{224}Ra with a Q-value of 12.102 MeV. With the experimental Q-value of 3.123 MeV, a larger half-life is shown at ^{212}Ra. This disagreement may be because of the sensitivity of half-life to the orbital angular momentum L [108] and also compatibility with the Q-value [109]. When isotopes of C are emitted from Ra isotopes, it is found from the Table 4 that there is remarkable agreement between the experimental and calculated half-lives of ^{222}Ra and ^{224}Ra with the calculated Q-value given in column 4. Again, with the experimental Q-value given in column 6 using the same UDL formalism, ^{224}Ra shows a small half-life, implying that the daughter nucleus ^{208}Pb is the obvious stable one. The decrease in half-lives is due to the double magicity (Z=82, N=126) of the well known ^{208}Pb daughter and the sensitivity of half-life to angular momentum L and Q-value. Also, with our calculated Q-value of 32.022 MeV, the same stable nucleus ^{208}Pb is obtained by emitting ^{12}C from ^{220}Ra. So our RMF model is suitable for explaining cluster radioactivity from heavy and superheavy nuclei, along with the study of ground state properties. In Table 5 we show the cluster decay half-life of O isotopes using the UDL and the universal formula. Both calculations show a small half-life for ^{224}Ra and hence the shell stabilization at ^{206}Hg is expected with the emission of ^{18}O. Again, the larger half-life is observed in ^{212}Ra with the emission of ^{16}O. So, shell stabilization may be found in the parent nucleus ^{212}Ra.

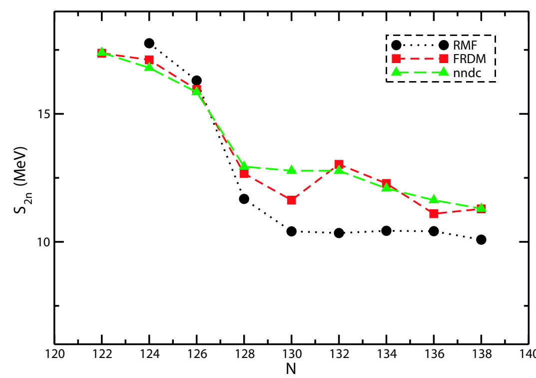

Fig. 3. (color online) Two-neutron separation energies S_{2n} (RMF) (circles) are compared with FRDM (squares) and experimental values (LHT) for the isotopes of Z = 88.

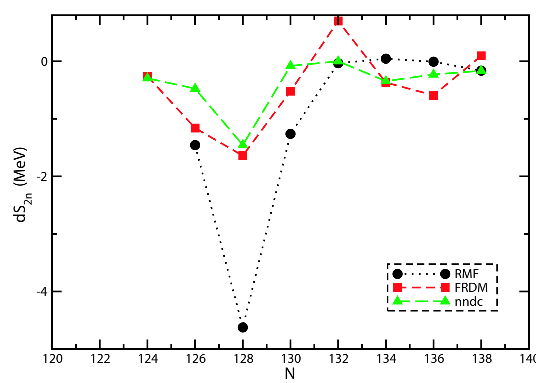

Fig. 4. (color online) The calculated differential variation of two-neutron separation energy dS_{2n} (RMF) (circles) compared with FRDM (squares) and experimental values (LHT) for the isotopes of Z = 88.

Table 2. Alpha decay half-lives from Ra isotopes.

parent nucleus	daughter nucleus	emitted cluster	calculated Q-value/MeV	VSS	Royer	UDL	Expt.
^{210}Ra	^{206}Rn	^{4}He	4.456	13.53	14.1	9.543	0.55
^{212}Ra	^{208}Rn	^{4}He	4.232	15.23	15.77	11.06	1.04
^{214}Ra	^{210}Rn	^{4}He	5.008	9.83	10.28	6.129	0.39
^{216}Ra	^{212}Rn	^{4}He	8.989	-5.77	-5.47	-8.07	-6.74
^{218}Ra	^{214}Rn	^{4}He	9.038	-5.89	-5.64	-8.21	-4.59
^{220}Ra	^{216}Rn	^{4}He	7.824	-2.47	-2.23	-5.12	-1.74
^{222}Ra	^{218}Rn	^{4}He	6.539	2.14	2.38	-0.95	1.58
^{224}Ra	^{220}Rn	^{4}He	5.336	7.91	8.15	4.25	5.49
^{226}Ra	^{222}Rn	^{4}He	4.526	13.02	13.26	8.87	10.70

Table 3. The decay half-lives of Be emission from Ra isotopes.

parent nucleus	daughter nucleus	emitted cluster	calculated Q-value/MeV	UDL (Calc.)	Q-value/MeV from Ref. [110]	UDL (Expt.)
^{210}Ra	^{202}Po	^{8}Be	4.571	86.7	13.443	20.04
^{212}Ra	^{204}Po	^{8}Be	3.123	120.31	13.201	20.84
^{214}Ra	^{206}Po	^{8}Be	3.934	99.16	13.341	20.30
^{216}Ra	^{208}Po	^{8}Be	8.729	42.4	15.814	12.60
^{218}Ra	^{210}Po	^{8}Be	14.522	16.31	17.662	7.93
^{220}Ra	^{212}Po	^{8}Be	12.218	24.37	15.701	12.82
^{222}Ra	^{214}Po	^{8}Be	9.688	36.38	13.849	18.37
^{224}Ra	^{216}Po	^{8}Be	7.177	54.68	12.102	24.74

Table 4. The decay half-lives of C emission from Ra isotopes.

parent nucleus	daughter nucleus	emitted cluster	calculated Q-value/MeV	UDL (Calc.)	Q-value/MeV from Ref. [110]	UDL (Expt.)	Expt.
^{210}Ra	^{198}Pb	^{12}C	17.34	41.79	26.511	21.65	
^{212}Ra	^{200}Pb	^{12}C	17.77	47.72	26.052	22.62	
^{212}Ra	^{198}Pb	^{14}C	18.25	50.73	22.839	34.51	
^{214}Ra	^{202}Pb	^{12}C	17.26	49.74	26.035	22.59	
^{214}Ra	^{200}Pb	^{14}C	18.14	51.10	23.324	33.01	
^{216}Ra	^{204}Pb	^{12}C	21.94	37.12	28.401	17.44	
^{216}Ra	^{202}Pb	^{14}C	22.26	36.13	26.205	25.28	
^{218}Ra	^{206}Pb	^{12}C	27.32	19.60	30.436	13.49	
^{218}Ra	^{204}Pb	^{14}C	28.20	20.61	28.741	19.45	
^{220}Ra	^{208}Pb	^{12}C	31.39	11.72	32.022	10.66	
^{220}Ra	^{206}Pb	^{14}C	33.65	10.12	31.039	14.77	
^{222}Ra	^{208}Pb	^{14}C	37.63	3.91	33.050	11.07	11.01
^{224}Ra	^{210}Pb	^{14}C	35.31	7.28	30.536	15.58	15.68
^{224}Ra	^{208}Pb	^{16}C	49.16	-8.87	26.882	26.11	
^{226}Ra	^{212}Pb	^{14}C	29.42	18.09	28.197	20.33	
^{226}Ra	^{210}Pb	^{16}C	30.03	18.79	24.703	31.83	

Table 5. The decay half-lives of O emission from Ra isotopes.

parent nucleus	daughter nucleus	emitted cluster	calulated Q-value/MeV	UDL	Univ
^{210}Ra	^{194}Hg	^{16}O	32.07	40.81	41.05
^{212}Ra	^{196}Hg	^{16}O	30.11	45.84	46.37
^{218}Ra	^{200}Hg	^{18}O	35.18	36.07	36.25
^{220}Ra	^{202}Hg	^{18}O	39.03	27.84	27.85
^{222}Ra	^{204}Hg	^{18}O	43.31	20.00	20.10
^{222}Ra	^{202}Hg	^{20}O	38.71	30.59	31.01
^{224}Ra	^{206}Hg	^{18}O	46.45	14.91	15.21
^{224}Ra	^{204}Hg	^{20}O	43.01	22.25	22.76
^{226}Ra	^{206}Hg	^{20}O	46.48	16.33	17.11
^{226}Ra	^{204}Hg	^{22}O	43.45	23.03	24.06

4 Conclusions

In conclusion, it has been found that the bulk properties, along with cluster emissions, provide a great contribution to the study of half-lives for Ra isotopes. The calculated half-lives of alpha and other characteristics pertaining to possible cluster emissions with the Q-values obtained from RMF model have been computed and tabulated. From the BE study of Ra isotopes it is found that the ^{214}Ra is the most stable element, with N=126. The differential variation of two-neutron separation energy in Fig. 4 shows a large dip at N=128, clearly showing shell/sub-shell stabilization. The results obtained for alpha particle emission from ^{218}Ra, ^{8}Be emission from ^{218}Ra, ^{12}C emission from ^{220}Ra and ^{18}O emission from ^{224}Ra indicate the shell is stabilized at the daughter nuclei, with the small half-lives of the parents. On the other hand, as long half-lives are obtained for parent nuclei such as ^{212}Ra and ^{224}Ra with the emission of alpha, ^{14}C, ^{16}O and ^{8}Be, this indicates possible shell/sub-shell closure at these nuclei. The present study of the exotic decays of radium isotopes may be helpful for future experiments in the mass region of A∼220.

References

1 A. Sǎndulescu, D. N. Poenaru, and W. Greiner, Sov. J. Part. Nucl., **11**: 528 (1980)
2 D. N. Poenaru, M. Ivascu, A. Sandulescu, and W. Greiner, J. Phys. G: Nucl. Part. Phys., **10**: L183 (1984)
3 D. N. Poenaru, M. Ivascu, A. Sandulescu, and W. Greiner, Phys. Rev. C, **32**: 572 (1985)
4 D. N. Poenaru, W. Greiner, A. Sandulescu, and M. Ivascu, Phys. Rev. C, **32**: 2198 (1985)
5 W. Greiner, M. Ivascu, D. N. Poenaru, and A. Sandulescu, Z. Phys. A, **320** 347 (1985)
6 Y. J. Shi and W. J. Swiatecki, Phys. Rev. Lett., **54**: 300 (1985)
7 G. A. Pik-Pichak and Sov. J. Nucl. Phys., **44**: 923 (1986)
8 G. Shanmugam and B. Kamalaharan, Phys. Rev. C, **38**: 1377 (1988)
9 B. Buck, A. C. Merchant, J. Phys. G: Nucl. Part. Phys., **15**: 615 (1989)
10 K. P. Santhosh, A. Joseph, Ind. J. of Pure & App. Phys., **42**: 806 (2004)
11 K. P. Santhosh, A. Joseph, Pramana J. Phys., **55**: 375 (2000)
12 S. Landowne, C. H. Dasso, Phys. Rev. C, **33**: 387 (1986)
13 M. Iriondo, D. Jerrestan, and R. J. Liotta, Nucl. Phys. A, **454**: 252 (1986)
14 R. Blendoaske, T. Fliessbach, and H. Walliser, Nucl. Phys. A, **464**: (75) (1987)
15 S. S. Malik, R. K. Gupta, Phys. Rev. C, **39**: 1992 (1989)
16 S. Kumar, R. K. Gupta, Phys. Rev. C, **55**: 218 (1997)
17 D. N. Poenaru, W. Greiner, in: C. Beck (Ed.), Clusters in Nuclei, in: Lecture Notes in Physics, vol., **818**: Springer, Berlin, p. 1 (2010)
18 H. J. Krappe, K. Pomorski, in: Theory of Nuclear Fission: A Textbook, in: Lecture Notes in Physics, vol., **838**: Springer, Berlin, p. 233 (2010)
19 D. N. Poenaru, R. A. Gherghescu, W. Greiner, Phys. Rev. Lett., **107**: 062503 (2011)
20 D. Ni, Z. Ren, T. Dong, C. Xu, Phys. Rev. C, **78**: 044310 (2008)
21 Z. Ren, C. Xu, Z. Wang, Phys. Rev. C, **70**: 034304 (2004) .
22 D. Ni, Z. Ren, Phys. Rev. C, **82**: 024311 (2010)
23 S. Hofmann et al, Eur. Phys. J. A, **10**: 5 (2001)
24 Yu. Ts. Oganessian et al, Phys. Rev. C, **74**: 044602 (2006); Phys, Rev, C, **70**: 064609 (2004)
25 G. Gamow, Z. Phys., **51**: 204 (1928)
26 E. U. condon, R. W. Gurney, Nature, **122**: 439 (1928)
27 H. Geiger, J. M. Nuttall, Philos. Mag., **22**: 613 (1911)
28 A. Sandulescu, D. N. Poenaru, W. Greiner, and J. H. Hamilton, Phys. Rev. Lett., **54**: 490 (1985)
29 H. J. Rose and G. A. Jones, Nature, **307**: 245 (1984)
30 S. Gales et al, Phys. Rev. Lett., **53**: 759 (1984)
31 P. B. Price et al, Phys. Rev. Lett., **54**: 297 (1985)
32 L. P. Gaffney et al, Nature, **497**: 199 (2013)
33 S. K. Ghorui, B. B. Sahu, C. R. Praharaj, and S. K. Patra, Phys. Rev. C, **85**: 064327 (2012)
34 B. B. Sahu, S. K. Singh, S. K. Patra, C. R. Praharaj, M. Bhuyan, Z. Naik, and S. K. Ghorui, Acta Physica. Polo. B, **43**: 451 (2012)
35 B. D. Serot and J. D. Walecka, Adv. Nucl. Phys., **16**: 1 (1986)
36 Y. K. Gambhir, P. Ring, and A. Thimet, Ann. Phys. (NY), **198**: 132 (1990)
37 H. Toki, Y. Sugahara, D. Hirata, B. V. Carlson, and I.Tanihata, Nucl. Phys. A, **524**: 633 (1991)
38 C. Qi, F.R. Xu, R. J. Liotta, R. Wyss, M. Y. Zhang, C. Asawatangtrakuldee, and D. Hu, Phys. Rev. C, **80**: 044326 (2009)
39 Z. Sheng, D. Ni, and Z. Ren, J. Phys. G, Nucl. Part. Phys., **38**: 055103 (2011)
40 T. T. Ibrahim, S. M. Perez, S. M. Wyngaardt, B. Buck, and A. C. Merchant, Phys. Rev. C, **85**: 044313 (2012) 062503 (2011) .
41 M. Balasubramaniam, R. K. Gupta, Phys. Rev. C, **60**: 064316 (1999)
42 J. L. Egido, L. M. Robledo, Nucl. Phys. A, **738**: 31 (2004)
43 L. M. Robledo, M. Warda, Int. J. Mod. Phys. E, **17**: 204 (2008)
44 L. M. Robledo, M. Warda, Int. J. Mod. Phys. E, **17**: 2275 (2008)
45 B. Buck, A. C. Merchant, and S. M. Perez, Nucl. Phys. A, **657**: 267 (1999)
46 K. P. Santhosh, R. K. Biju, and A. Joseph, J. Phys. G, Nucl. Part. Phys., **35**: 085102 (2008)
47 K. P. Santhosh, S. Sahadevan, B. Priyanka, and M. S. Unnikrishnan, Nucl. Phys. A, **882**: 49 (2012)
48 K. P. Santhosh, R. K. Biju, S. Sahadevan, and A. Joseph, Phys. Scr., **77**: 065210 (2008)
49 K. P. Santhosh, Phys. Scr., **81**: 015203 (2010)
50 D. N. Poenaru, R. A. Gherghescu, and W. Greiner, Phys. Rev. C, **83**: 014601 (2011)
51 S. S. Malik, R. K. Gupta, Phys. Rev. C, **39**: 1992 (1989)
52 D. N. Basu, Phys. Rev. C, **66**: 027601 (2002)
53 R. K. Gupta, S. Singh, R. K. Puri, W. Scheid, Phys. Rev. C, **47**: 561 (1993)
54 S. Kumar, R. K. Gupta, Phys. Rev. C, **49**: 1922 (1994)
55 K. P. Santhosh, S. Sahadevan, B. Priyanka, and M. S. Unnikrishnan, Nucl. Phys. A, **882**: 49 (2012)
56 T. R. Routray, J. Nayak, and D. N. Basu, Nucl. Phys. A, **826**: 223 (2009)
57 G. Sawhney, M. K. Sharma, R. K. Gupta, Phys. Rev. C, **83**: 064610 (2011)
58 A. Soylu, Y. Sert, O. Bayrak, and I. Boztosun, Eur. Phys. J. A, **48**: 128 (2012)
59 K. P. Santhosh, A. Joseph, and Pramana J. Phys., **59**: 679 - 684 (2002)
60 A. Soylu and S. Evlice, Nucl. Phys. A, **936**: 59 (2015)
61 K. P. Santhosh, T. Ambily, S. Sabina, R. K. Biju, and A. Joseph, Proc. Nat. Symp. Nucl. Phys. (India), **1**: 33 (2009)
62 K. P. Santhosh, S. Sabina, B. Priyanka, M. S. Unnikrishnan, G. J. Jayesh, and R. K. Biju, Proc. DAE Symp. Nucl. Phys. (India), **56**: 298 (2011)
63 G. A. Lalazissis et al, Phys. Rev. C, **55**: 540 (1997)
64 B. G. Todd-Rutel et al, Phys. Rev. Lett., **95**: 122501 (2005)
65 V. E. Viola, Jr. and G. T. Seaborg, J. Inorg. Nucl. Chem., **28**: 741 (1966)
66 G. Royer, Nucl. Phys. A, **848**: 279 (2010)
67 J. M. Dong, et al, Nucl. Phys. A, **832**: 198 (2010)
68 C. Qi, F. R. Xu, R. J. Liotta, and R. Wyss, Phys. Rev. Lett., **103**: 072501 (2009)
69 C. Qi, F. R. Xu, R. J. Liotta, R. Wyss, M. Y. Zhang, C. Asawatangtrakuldee, and D. Hu, Phys. Rev. C, **80**: 044326 (2009)

70 L. I. Schiff, Phys. Rev., **84**: 1 (1951)
71 M. H. Johnson and E. Teller, Phys. Rev., **98**: 783 (1955)
72 H. P. Durr and E. Teller, Phys. Rev., **101**: 494 (1956)
73 J. D. Walecka, Ann. Phys. (N.Y.), **83**: 491 (1974)
74 C. J. Horowitz, and B. D. Serot, Nucl. Phys. A, **368**: 503 (1981)
75 T. Gonzales-Llarena, J. L. Egido, G. A. Lalazissis, and P. Ring, Phys. Lett. B, **379**: 13 (1996)
76 W. Pannert, P. Ring, and J. Boguta, Phys. Rev. Lett., **59**: 2420 (1986)
77 Y. K. Gambhir, P. Ring, and A. Thimet, Ann. Phys. (N.Y.) , **198**: 132 (1990)
78 J. Boguta, A. R. Bodmer, Nucl. Phys. A , **292**: 413 (1977)
79 S. K. Patra and C. R. Praharaj, Phys. Rev. C, **44**: 552 (1991)
80 M. Del Estal, M. Centelles, X. Vinas, and S. K. Patra, Phys. Rev. C **63**: 024314 (2001)
81 G. Gangopadhyay, Phys. Rev. C, **59**: 2541 (1999)
82 G. A. Lalazissis and S. Raman, Phys. Rev. C, **58**: 1467 (1998)
83 J. Meng et al, Prog. Part. Nucl. Phys., **57**: 470 (2006)
84 J. Konig, and P. Ring, Phys. Rev. Lett., **71**: 3079 (1993)
85 Z. Z. Ren, Phys. Rev. C, **65**: 051304(R) (2002)
86 S. Das and G. Gangopadhyay, J. Phys. G: Nucl. Part. Phys. **30**: 957 (2004)
87 H. F. Zhang et al, Phys. Rev. C, **71**: 054312 (2005)
88 J. Q. Li et al, Phys. Rev. C, **65**: 064305 (2002)
89 Renli Xu, Chen Wu, and Zhongzhou Ren, J. Phys. G: Nucl. Part. Phys., **39**: 085107 (2012)
90 Renli Xu, Chen Wu, Guoliang Ma, Deqing Fang, and Zhongzhou Ren Phys. Rev. C, **87**: 014335 (2012)
91 B. B. Sahu, S. K. Agarwalla, and S. K. Patra, Phys. Rev. C, **84**: 054604 (2011)
92 D. G. Madland and J. R. Nix, Nucl. Part. Phys. A, **476**: 1 (1981)
93 P. Moller and J. R. Nix, At. Data Nucl. Data Tables **39**: 213 (1988)
94 G. A. Lalazissis, et al., Phys. Rev. C, **60**: 014310 (1999)
95 A. Sobiczewski, Z. Patyk, S. Cwiok, Phys. Lett. B, **224**: 1 (1989)
96 A. M. Lane and R. G. Thomas, Rev. Mod. Phys., **30**: 257 (1958)
97 R. G. Lovas, R. J. Liotta, A. Insolia, K. Varga, and D. S. Delion, Phys. Rep., **294**: 265 (1998)
98 D. S. Delion, R. J. Liotta, and R. Wyss, Phys. Rev. Lett., **96**: 072501 (2006)
99 C. Qi, F. R. Xu, R. J. Liotta, and R. Wyss, Phys. Rev. Lett., **103**: 072501 (2009)
100 G. Royer, J. Phys. G. Nucl. Part. Phys., **26**: 1149 (2000)
101 P. Mller, J. R. Nix, W. D. Wyers, and W. J. Swiaterecki, At.Data and Nucl. Data Tables, **59**: (1995) 185 ; P. Mller, J. R. Nix, and K. -L. Kratz, At. Data and Nucl. Data Tables, **66**: 1318 (1997)
102 http://www.nndc.bnl.gov.
103 S.Iversen, H.Nann, A.ObstKamal, K.Seth, N.Tanaka, C.L.Morris, H.A.Thiessen, K.Boyer, W.Cottingame, C.Fred Moore, R.L.Boudrie, D.Dehnhard, Phys, Lett, B, **82**: 51 (1979)
104 W. Hirt, Nuclear Physics B, **9**: 447, (1969)
105 B. Sahu et. al., Phy. Rev. C, **77**: 024604 (2008)
106 S.A. Changizi, C. Qi, Nucl. Phys. A, **951**: 97 (2016)
107 F. Iachello, and N. V. Zamfir, Phys Rev. Lett., **92**: 212501 (2004)
108 Bidhubhusan Sahu, S. K. Agarwalla, and S. K. Patra, Phys. Rev. C, **84**: 054604 (2011)
109 R. D. Page et al., Phys. Rev. C, **75**: 061302(R) (2007)
110 G. Audi, A. H. Wapstra, C. Thivault, Nucl. Phys. A, **729**: 337 (2003)